JOURNAL OF GEOPHYSICAL RESEARCH, VOL. 107, NO. B11, 2292, doi:10.1029/2001JB000743, 2002

# Neotectonic modeling of the Ibero-Maghrebian region

Ana M. Negredo,[1] Peter Bird,[2] Carlos Sanz de Galdeano,[3] and Elisa Buforn[1]

Received 12 July 2001; revised 10 April 2002; accepted 9 May 2002; published 14 November 2002.

[1] Thin-shell finite element techniques have been applied to model the neotectonics of the Ibero-Maghrebian region, in the westernmost Mediterranean. This region is characterized by a complex seismotectonic pattern and moderate seismic activity associated with the convergence between Africa and Eurasia. We compare two end-member models using different fault networks. Model predictions, including anelastic strain rates, vertically integrated stresses and velocity fields, are compared to the seismicity map and to data on directions of maximum horizontal compression. Best results are obtained assuming a low fault friction coefficient (0.05) and when the Betics and Rif are modeled as parts of the same arc-shaped chain. The highest predicted fault slip rates are in the Tell mountains. Farther to the west, fault slip is more homogeneously distributed over the Betic-Rif chain, Gulf of Cadiz, and Alboran Sea, indicating a diffuse geometry of the plate boundary in this area. The areas of highest predicted strain rates coincide with the most seismically active regions, located in northern Algeria and northeastern Morocco. Our best model also reproduces a major change of the stress regime, from thrusting in the east (Tell mountains) to predominantly strike-slip and normal faulting in the west (Betic-Rif chain and Alboran Sea). The Alboran basin is shown to be undergoing significant internal transpression and therefore cannot be considered as a rigid microplate. The western part of the Alboran Sea and surrounding areas are being extruded to the WNW with respect to Iberia. *INDEX TERMS:* 8107 Tectonophysics: Continental neotectonics; 1206 Geodesy and Gravity: Crustal movements—interplate (8155); 8123 Tectonophysics: Dynamics, seismotectonics; 8164 Tectonophysics: Evolution of the Earth: Stresses—crust and lithosphere; 1242 Geodesy and Gravity: Seismic deformations (7205); *KEYWORDS:* neotectonics, plate boundary, stress, strain rate, Ibero-Maghrebian region

**Citation:** Negredo, A. M., P. Bird, C. Sanz de Galdeano, and E. Buforn, Neotectonic modeling of the Ibero-Maghrebian region, *J. Geophys. Res.*, *107*(B11), 2292, doi:10.1029/2001JB000743, 2002.

## 1. Introduction

[2] The study area includes the southern part of the Iberian Peninsula, the western Mediterranean, and the northwestern part of Africa and is located in the western part of the plate boundary between Eurasia and Africa. Moderate seismicity is associated with convergence between these plates and is distributed over a wide area of deformation, as would be expected in a continent-continent collision. Figure 1 shows the seismicity of the region during the instrumental period (1910–1999), restricted to magnitudes equal or larger than 3.5 to avoid regional bias, taken from the catalogue provided by the Instituto Geográfico Nacional of Spain. We have performed a completeness analysis of this seismic catalogue and have obtained a value of 3.5 for the magnitude of completeness. Earthquakes in the Tell region have larger magnitudes and shorter recurrence periods [*Bezzeghoud et al.*, 1996] than those located farther to the west. Although most earthquakes are at shallow depth ($h < 40$ km), significant seismic activity is present at intermediate ($40 < h < 130$ km) and very great ($\cong$650 km) depths [*Chung and Kanamori*, 1976; *Udías et al.*, 1976; *Grimison and Chen*, 1986; *Buforn et al.*, 1991; *Morales et al.*, 1997].

[3] Although historical seismicity studies report the occurrence of large earthquakes in the south of Iberia, instrumental magnitudes larger than 5.5 have mostly occurred in the Gulf of Cadiz and north of Africa. The largest recent earthquakes were the Gorringe Bank (28 February 1969, $M_s$ = 8.0) and El-Asnam, Algeria (10 October 1980, $M_s$ = 7.3), events. The largest earthquake in the Gulf of Cadiz (15 March 1964) was of magnitude 6.2. Also, the Mediterranean coast of Morocco was affected on 26 May 1994, by a destructive earthquake ($M_w$ = 5.8) near the city of Alhoceima (at the eastern end of the Rif belt).

[4] Several studies point out the complexities of the seismotectonic pattern [*Buforn et al.*, 1995; *Galindo-Zaldívar et al.*, 1999]. Large thrust earthquakes show a consistent N-S to NW-SE orientation of *P* axes, corresponding to the plate convergence direction. This horizontal compression coexists with E-W to NE-SW-directed horizontal tension in the Betics, Alboran Sea and northern Morocco. Figure 2 shows a compilation of data on the directions of maximum horizontal compression. Most data (63) come from the

[1]Departamento de Geofísica, Facultad de Física, Universidad Complutense de Madrid, Madrid, Spain.
[2]Department of Earth and Space Sciences, University of California, Los Angeles, California, USA.
[3]Instituto Andaluz de Ciencias de la Tierra, Consejo Superior de Investigaciones Científicas-Universidad de Granada, Granada, Spain.


0148-0227/02/2001JB000743$09.00

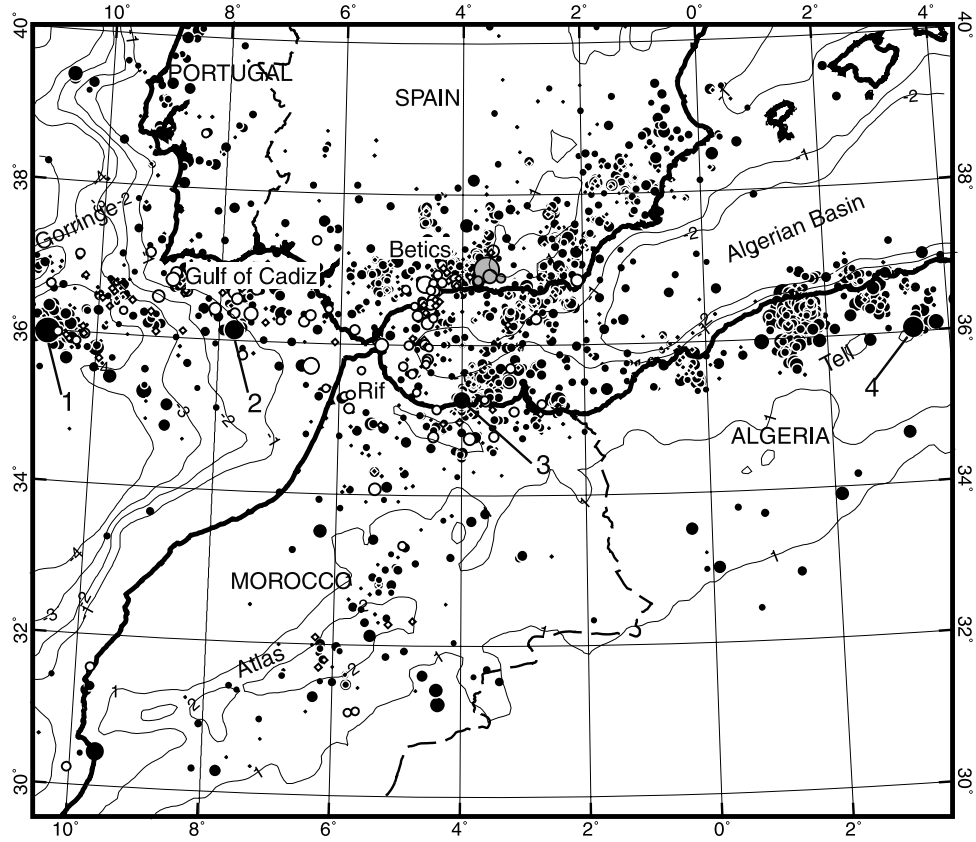


**Figure 1.** Topographic map (generated from the ETOPO5 data set) showing the seismicity distribution in the study area (Instituto Geográfico Nacional data file, 1910–1999, $M \geq 3.5$). Solid, white, and gray circles represent shallow ($h < 40$ km), intermediate ($40 \leq h \leq 130$ km), and deep earthquakes ($h > 130$ km), respectively. The four earthquakes mentioned in the text are indicated with numbers 1 (28 February 1969, $M_s = 7.8$), 2 (15 March 1964, $M = 6.2$), 3 (26 May 1994, $M_w = 5.8$), and 4 (10 October 1980, $M_s = 7.3$). A geometric conic projection has been used, as in the rest of figures.

World Stress Map data set by *Zoback* [1992], updated in 2000 [*Mueller et al.*, 2000]. We have added 55 data from published studies of focal mechanisms of events with magnitude 4.0 or greater [e.g., *Bezzeghoud and Buforn*, 1999]. The assignment of data quality, varying from A to E, is based on the same criterion as used by *Zoback* [1992].

[5] Two recent neotectonic studies using distinct modeling methods (the thin sheet and thin shell approaches of *Jiménez-Munt et al.* [2001a, 2001b]) have investigated the geometry and strength of the Africa-Eurasia plate boundary in the Azores-Alboran region, as well as the most plausible boundary conditions. They suggest a bifurcation of the plate boundary east of the Gorringe Bank toward the Alboran region, with one branch in south Iberia and the other one in north Africa. However, as Jiménez-Munt et al. point out, results concerning the tectonics of the Alboran domain are very qualitative because this region is close to the boundary of their study area. Furthermore, the only fault zones considered in the Alboran region are the Betic and Rif thrust fronts and only stress data west of 5°W (Gibraltar) were used in scoring model predictions.

[6] We carry out a detailed neotectonic study of the Alboran region and surrounding areas, including major fault zones potentially active in south Iberia, the Alboran Sea and northern Morocco. Another significant novelty of this study is that the model domain extends to the east to include the young oceanic Algerian basin and the Tell mountains in northern Algeria, which is the most seismically active part of the western Mediterranean region. By including these regions we will be able to compare the deformational styles associated with continent-continent and continent-young ocean convergence. The main purpose of this study is to model the present-day patterns of velocity, stress and strain rate to improve the understanding of the tectonic processes presently active in the Ibero-Maghrebian area. We also intend to better constrain the geometry of the plate boundary in the transition from the Atlantic to the Mediterranean Sea. Moreover, this neotectonic modeling is intended to provide some estimates of slip rates of major fault zones and therefore evaluate their relative long-term seismic hazard.

## 2. Geological Setting and Evolution

[7] The most significant geologic features related to interplate processes are the Betic, Rif, and Tell cordilleras, which may link across the Gibraltar Arc. They constitute the westernmost end of the Alpine orogenic belt in southern Europe and limit the Alboran Sea and the Algerian basin.

[8] This orocline results from the Cretaceous to Paleogene collision of the Eurasian and African plates. Structural contacts between thrust sheets and nappes generally dip to the south in the Betics and to the north in the Rif; that is,

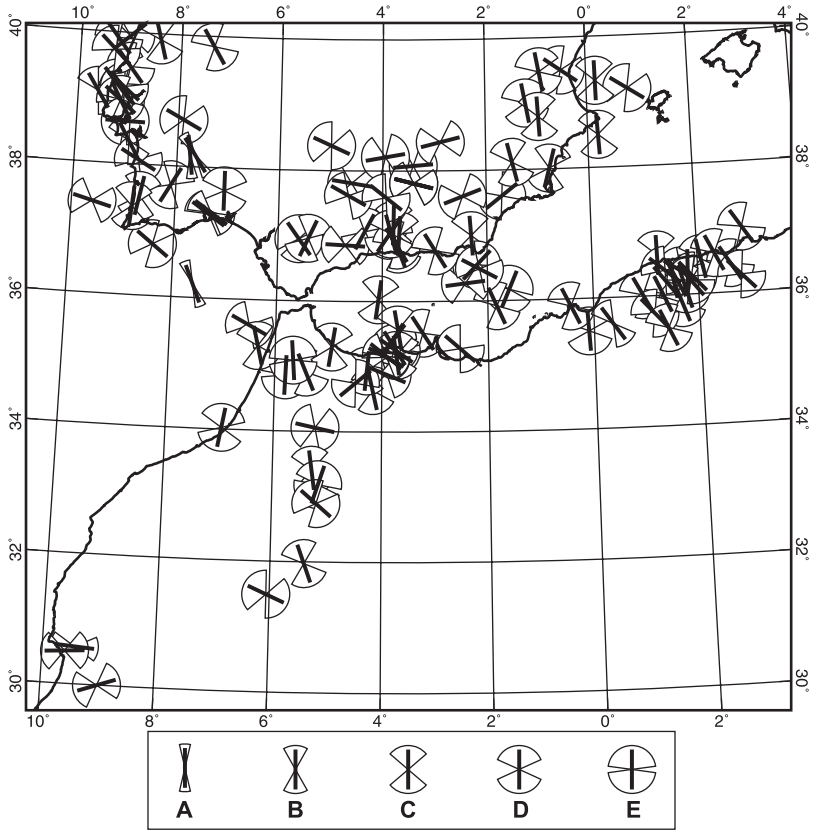


**Figure 2.** Directions and uncertainty ranges of the most compressive horizontal principal stress. The key associates A, B, C, D, E qualities with pie-wedge symbols of different sizes. Most data (63) come from the World Stress Map project [*Zoback*, 1992; *Mueller et al.*, 2000], and 55 additional data come from published focal mechanism analyses of earthquakes of magnitude 4.0 or greater [e.g., *Bezzeghoud and Buforn*, 1999].

toward a central ''internal zone.'' The internal zone of the Betic-Rif orogen is common to both cordilleras and consists of metamorphic complexes showing N-S continuity below the Alboran Sea; these units define the so-called Alboran domain. Mountain ranges in the internal zone are separated by Neogene intramontane basins. The intermediate ''flysch zone'' consists of nappes of Early Cretaceous to early Miocene sediments, which originally overlaid a very thin continental or oceanic crust. The ''external zones'' are formed of Mesozoic and Tertiary sedimentary rocks from the former South Iberian and Maghrebian continental paleomargins (Figure 3).

[9] During the early and middle Miocene the Alboran domain underwent extension and thinning of a previously thickened crust. The most striking feature is that extension in the Alboran domain was active simultaneously with thrusting

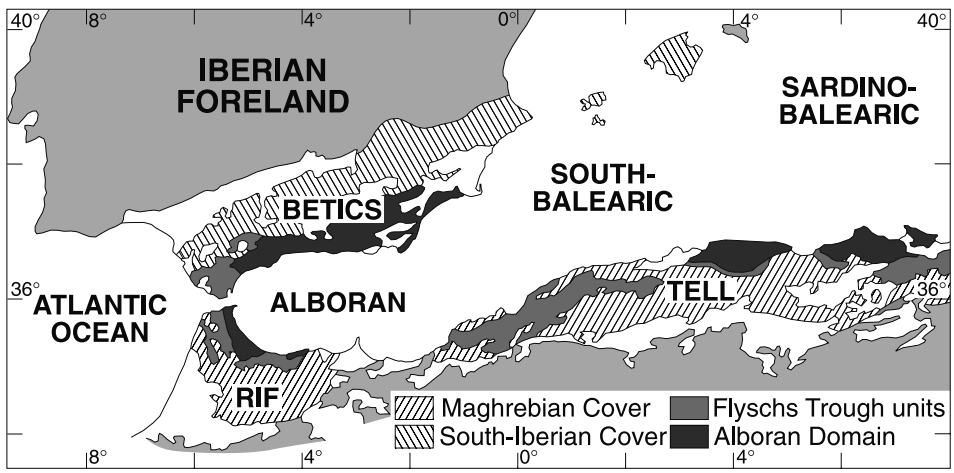


**Figure 3.** Simplified geologic map showing the main crustal domains of the Betic-Rif orogen and Tell mountains [from *Comas et al.*, 1999].

and shortening of the external zones, which were deformed into a thin-skinned fold and thrust belt [e.g., *Frizon de Lamotte*, 1987; *García-Dueñas et al.*, 1988, 1992; *Comas et al.*, 1992]. Simultaneously, important westward displacements, relative to the Iberian and African forelands, occurred in the internal zone of the Betic-Rif orogen [e.g., *Andrieux et al.*, 1971; *Sanz de Galdeano*, 1990]. The Gibraltar Arc is thought to be a result of westward overthrusting of the Alboran domain onto Iberian and Maghrebian crust [*Balanyá and García-Dueñas*, 1987]. Several geodynamic models have been proposed to explain the origin of the Alboran basin within an overall compressional setting: rapid westward motion of a rigid Alboran microplate [*Andrieux et al.*, 1971; *Leblanc and Olivier*, 1984]; subduction roll-back combined with back-arc extension [e.g., *Royden*, 1993; *Lonergan and White*, 1997]; convective removal of lithospheric mantle [*Platt and Vissers*, 1989; *Vissers et al.*, 1995], or asymmetric delamination of lithospheric mantle [e.g., *García-Dueñas et al.*, 1992; *Docherty and Banda*, 1995; *Seber et al.*, 1996; *Mézcua and Rueda*, 1997; *Calvert et al.*, 2000].

[10] Extension in the Alboran domain ceased by late Miocene. Ongoing plate convergence then produced folding, thrusting, strike-slip faults and tectonic inversion of previous normal faults. This orogeny was accompanied by uplift and progressive emersion of some peripheral marine depocenters [e.g., *Sanz de Galdeano and Vera*, 1992].

## 3. Methodology

[11] We model the neotectonics of the Ibero-Maghrebian region with the finite element program SHELLS [*Kong*, 1995; *Kong and Bird*, 1995; *Bird*, 1999]. The lithosphere is approximated as a spherical thin shell of variable thickness. The two-dimensional finite element grid consists of continuum and fault elements. Only the horizontal components of the momentum equation are solved and the angular velocity is assumed to be independent of depth in the lithosphere. The method has some characteristics of three-dimensional methods because it performs volume integrals of density and strength in a lithosphere of variable crustal and mantle lithosphere thickness.

[12] Since the program is designed for neotectonic modeling, it neglects transient effects and solves for time-averaged steady velocities, fault slip rates, and stresses. Furthermore, this method solves for anelastic deformation, and so elastic strain, earthquake cycles, and other transient phenomena are not included. All the outputs should be considered as averages over several seismic cycles.

[13] The models assume a nonlinear rheology. At many test points throughout the volume of the lithosphere, the deviatoric stress tensor is calculated using both frictional sliding and dislocation creep flow laws. The mechanism giving the lower maximum shear stress is assumed to be dominant at that point. The fault friction coefficient is assumed to be 0.85 in continuum elements; but a reduced value, which will be varied from one model to another, is used in fault elements. We have used the following dislocation creep (power law) rheology [*Kirby*, 1983]:

$$\tilde{\sigma} = \left[ 2A \left( 2\sqrt{-\dot{\varepsilon}_1\dot{\varepsilon}_2 - \dot{\varepsilon}_2\dot{\varepsilon}_3 - \dot{\varepsilon}_3\dot{\varepsilon}_1} \right)^{(1-n)/n} \exp\left( \frac{B + Cz}{T} \right) \right] \tilde{\dot{\varepsilon}}, \quad (1)$$

where $\tilde{\sigma}$ is the deviatoric stress tensor, $\tilde{\dot{\varepsilon}}$ is the anelastic strain rate tensor, $T$ is absolute temperature, and $z$ is depth. The values adopted for the rheologic parameters $A$, $B$, and $C$ are different for the crust and mantle lithosphere. In order to evaluate how sensitive the model results are to changes in the rheologic parameters we have tested different values of the crustal creep activation energy $Q$, and therefore different extents of coupling between the upper crust and the upper mantle. The parameter $B$ in the crust is given by $Q/(nR)$, where $R$ is the gas constant. The creep activation energy $Q$ is varied between 100 and 400 kJ mol$^{-1}$, which is the approximate range of experimental results for plausible lower crustal rocks [*Kirby*, 1983]. Values of $Q$ and $A$ are not varied independently, but following the relationship obtained in neotectonic studies of California by *Bird and Kong* [1994] to fit the depth of brittle-ductile transition:

$$\log_{10} A = 12.2 - (2.8 \times 10^{-5})Q. \quad (2)$$

The mantle rheology is based on the studies of olivine deformation summarized by *Kirby* [1983]. The rheologic parameters adopted for the crust-mantle are $A = 4 \times 10^6/9.5 \times 10^4$ Pa s$^{1/3}$; $B$ = 8000/18,314 K; $C$ = 0/0.017 K/m; $n$ = 3 (for both layers). These values are shown below to give the best results when scoring model predictions against data.

[14] In the calculation of the frictional strength, we assume no cohesion, hydrostatic pore pressure, and we correct normal stresses by these estimated pore pressures to obtain effective normal stresses. The modeling approach assumes local isostasy, so vertical normal stress is assumed to be lithostatic and no flexural effects are considered.

## 4. Input Data

### 4.1. Grid Geometry and Boundary Conditions

[15] In this paper we focus on the comparison of two sets of models that differ in the set of faults considered. Figure 4 shows the finite element grid created for the first of these model sets, in which the selection of faults was very conservative, and no effort was made to create a connected plate boundary system. The grid consists of 2410 continuum elements and 291 fault elements. We have only included mapped fault zones thought to be active or potentially active. (Some fault elements do not represent individual faults, but zones of faults.) We assign a dip to each fault element. Where we do not have geologic or geophysical data providing an estimate for dip, we tentatively assign a dip of 25° for thrusts, 65° for normal faults, and 90° for strike-slip faults. Dip assignment does not determine the character of the solution: only vertical faults are forced to have strike-slip motion; all dipping faults may slip in any sense. Also, any fault which is not sufficiently stressed may remain inactive.

[16] Faults in southern Iberia were digitized from the seismotectonic map created by the *Instituto Geográfico Nacional* [1992]. The N60–70°E striking Cadiz-Alicante zone of subparallel faults has been simplified in the model and is represented by a long continuous fault. This zone of faults, together with the E-W trending faults farther to the south, moved as dextral strike-slip faults during the early and middle Miocene to accommodate relatively westward motion of the internal zone of the Betic chain [*Sanz de*

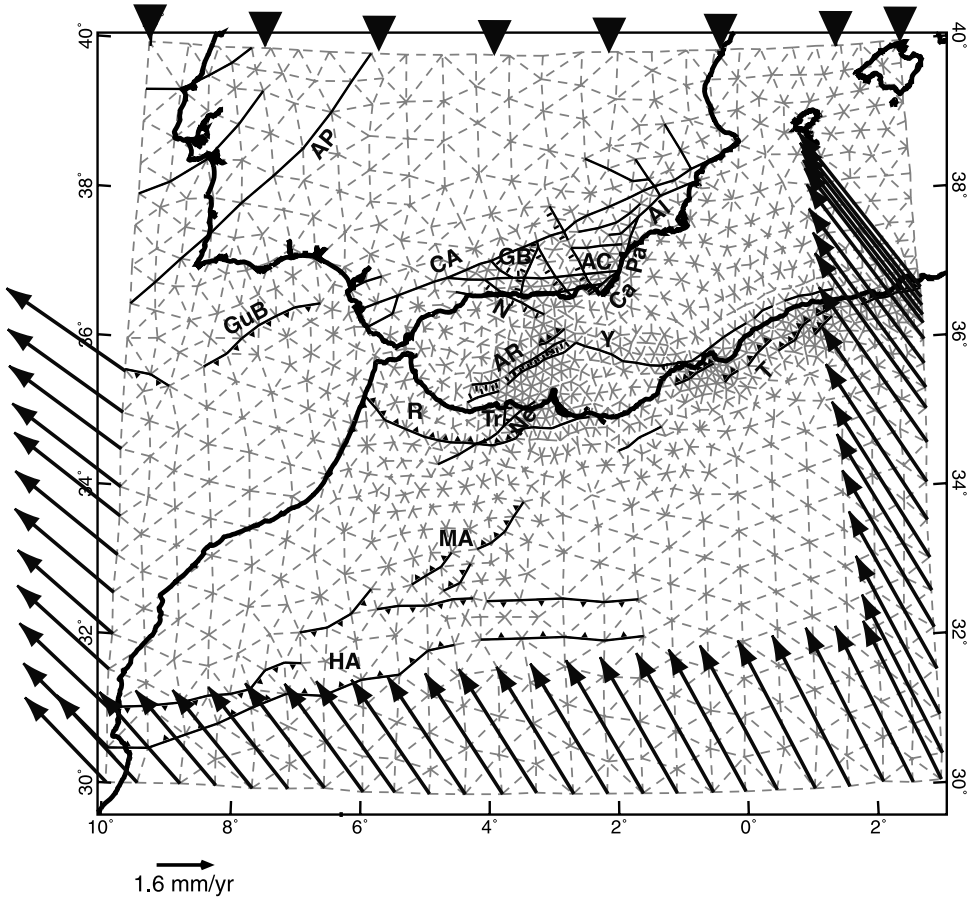


**Figure 4.** Finite element grid used for model set 1. Dashed and heavy lines represent continuum and fault elements, respectively. Different tick marks indicate assigned fault dip: triangle, 25°; straight, 65°; none, 90°. Names of fault zones are AC, Alpujarran corridor; Ca-Pa-Al, Alhama-Palomares-Carboneras; AP, Alentejo-Plasencia; AR, Alboran Ridge; CA, Cadiz-Alicante; GB, Granada Basin; GuB, Guadalquivir Bank; HA, High Atlas; N, Nerja; MA, Middle Atlas; Ne, Nekor; R, Rif; T, Tell; Tr, Trougout; Y, Yussuf. Velocity boundary conditions are shown with arrows: the northern boundary is fixed in the Eurasian reference frame, and the velocity of the Africa plate is applied to the southwestern, southeastern and southern boundaries.

*Galdeano*, 1996]. Despite this important motion during the past, the Cadiz-Alicante fault zone does not seem to be active in the present-day situation and only local dip-slip (mainly reverse) motions are recognized [*Sanz de Galdeano*, 1983]. (Generally, we have preferred to include all major fault zones, such as the Cadiz-Alicante system, although we do not know whether they constitute planes of weakness any longer. Omitting these dubious faults could lead to the elimination of important degrees of freedom. Furthermore, if they are not favorably oriented, they will remain inactive, and the solution will be equivalent to one which did not include them.)

[17] Fault traces in the Alboran Sea are taken from *Comas et al.* [1999]. On the basis of seismicity distribution and seismic reflection profiles [e.g., *Watts et al.*, 1993; *Alvarez-Marrón*, 1999], we have selected mapped faults showing evidence of neotectonic activity. Some authors [e.g., *De Larouzière et al.*, 1988] have proposed the existence of a lithospheric strike-slip fault zone extending from southeastern Spain, across the Alboran Sea, through the eastern Rif, and possibly to the Middle Atlas. However, seismic reflection data [e.g., *Watts et al.*, 1993] provide no evidence for a continuous shear zone offshore; therefore we have preferred not to include this hypothetical trans-Alboran shear zone in our models. Farther to the west, in the central part of the Gulf of Cadiz, we have included a reverse fault following the Guadalquivir Bank, an elongated uplifted zone characterized by a large gravity signature (up to 120 mGal [*Gràcia et al.*, 2000]) and significant seismicity (Figure 1). This fault, mapped in new multichannel seismic profiles [*Gràcia et al.*, 2000], probably formed during the extensional period in the Mesozoic. The strong tilting of overlying sedimentary units suggests a recent tectonic emplacement of the Guadalquivir Bank. Although of similar orientation, this fault should not be confused with the front of the olistostromes, which are units characterized by chaotic seismic reflections [*Tortella et al.*, 1997; *Maldonado et al.*, 1999] suggesting gravitationally emplaced foreland sediments.

[18] Fault traces in the Atlas and northeastern Morocco were digitized from the 1:500,000 geologic map of *Choubert et al.* [1955]. The thrust fault introduced in the area of

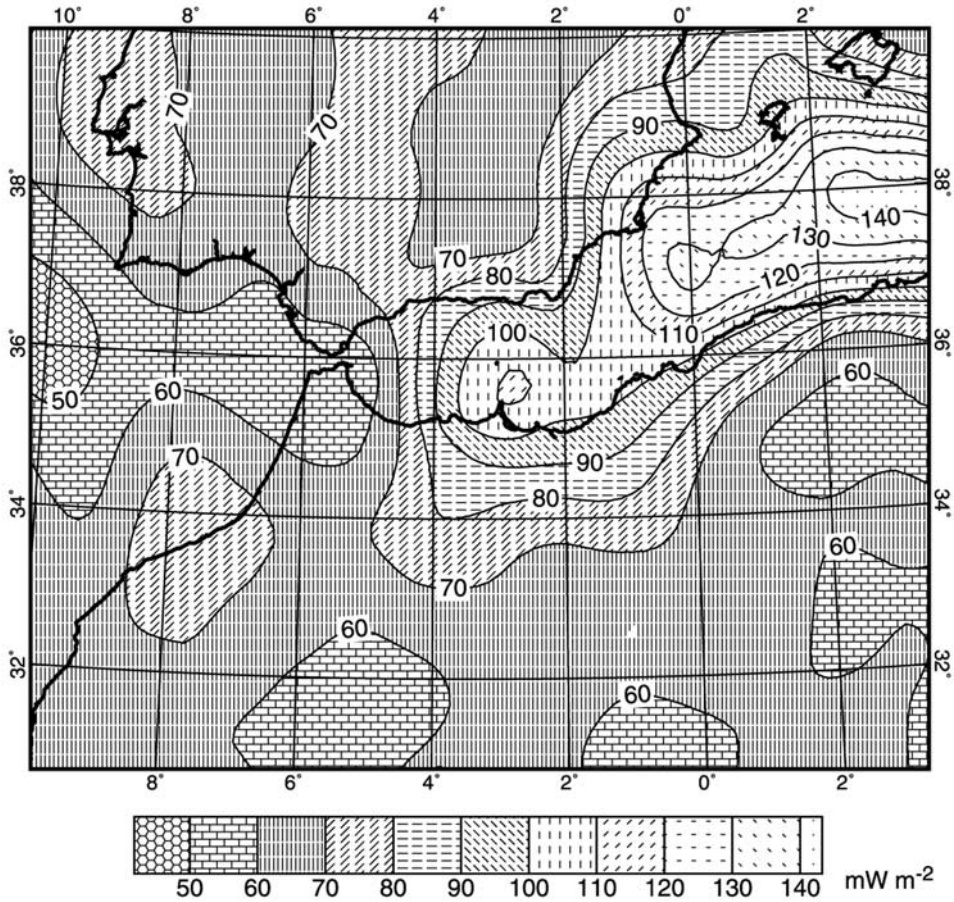


**Figure 5.** Surface heat flow distribution (see text for description of data sources) used to calculate lithosphere thickness. The most remarkable feature is the heat flow increase from the Gibraltar Arc to the Alboran Sea and Algerian basin.

the Rif chain should be interpreted as a simplification of all Rifean thrusts. This idealized structure roughly follows the limit between the external and the Pre-Rif units.

[19] The fault set in the Tell mountains is simplified from *Meghraoui et al.* [1996]. The main seismogenic structures are NE-SW-striking thrust faults dipping to the NW, such as the El-Asnam and Tipasa faults. They often exhibit a right-lateral en echelon pattern, which suggests the occurrence of E-W strike-slip faults at depth, or at least a dextral component to the thrusting.

[20] The boundary conditions are schematically shown in Figure 4. We assume that regions outside the southern boundary of the model are rigid parts of the Africa plate. We use the pole and rotation velocity of Africa obtained by *Argus et al.* [1989] to impose boundary conditions reproducing the rotation of Africa with respect to a fixed Eurasia plate. In some models, we have also tested the rotation pole and velocity obtained in the global plate model NUVEL-1 [*DeMets et al*, 1990]. Consistently with the results obtained in neotectonic models of the Azores-Gibraltar zone [*Jiménez-Munt et al.*, 2001a], we have obtained a better fit of the observations when applying the *Argus et al.* [1989] pole. The northern boundary is fixed as the velocity reference frame. We allow motion of the northeastern and northwestern boundaries, but with the difference that the northeastern "free" boundary has normal tractions based on local lithostatic pressure, whereas the northwestern one has normal tractions based on lithostatic pressure from the mid-Atlantic spreading rise.

### 4.2. Heat Flow

[21] The assumed heat flow distribution used to calculate lithospheric thickness is shown in Figure 5. This distribution has been obtained by smoothing and interpolating data of *Fernàndez et al.* [1998] for the Spanish mainland, of *Polyak et al.* [1996] for the Alboran Sea, and of *Pollack et al.* [1993] for the other continental zones. The most remarkable feature of surface heat flow distribution is the increase from the Gibraltar Arc to the Algerian basin, where we find high values typical of a young oceanic lithosphere.

### 4.3. Lithospheric Structure

[22] The topography and heat flow distribution, together with the approximation of local isostasy, permit us to find a continuous distribution of crustal and mantle lithosphere thickness. These thicknesses are calculated by an iterative method to attain both local isostasy with respect to a typical mid-oceanic ridge, and a fixed temperature at the base of the lithosphere. The crustal-mantle parameters used in these calculations are: densities of 2800/3386 kg $m^{-3}$ at 0 K,

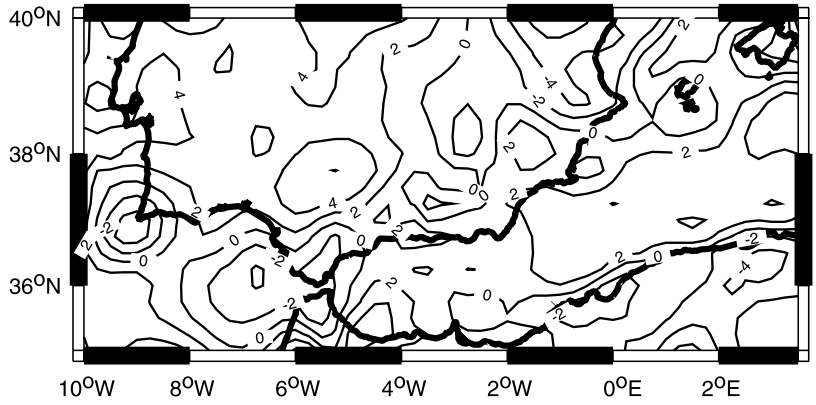


**Figure 6.** Distribution of discrepancies (in km) between crustal thickness derived from wide-angle seismic studies (see references in the text) and the values computed in this study.

volumetric thermal expansion coefficients of $0/3.5 \times 10^{-5}$ $K^{-1}$, a constant thermal conductivity of 3 W $m^{-1}$ $K^{-1}$ and constant radioactive heat production of $7.91 \times 10^{-7}$ W $m^{-3}$ in the crust (negligible in the mantle) and a temperature of 1300°C at the base of the lithosphere.

[23] The resulting crustal thickness distribution has a thickening under the Betic-Rif belt and Atlas cordillera. This contrasts with crustal thinning under the Alboran Sea, Algerian basin and Gulf of Cadiz. This pattern of crustal thickness is in good agreement with that derived from seismic refraction data. Figure 6 shows the distribution of crustal thickness differences between the values derived from deep seismic wide-angle studies [e.g., *Hatzfeld and The Working Group for Deep Seismic Sounding*, 1978; *Banda*, 1988; *Banda et al.*, 1993] and those computed in this modeling assuming a crustal density value of 2800 kg $m^{-3}$. Discrepancies do not exceed 4 km. We have performed sensitivity tests showing that varying the crustal thickness by this amount does not significantly modify the dynamic results. When crustal density is increased to 2850 kg $m^{-3}$ maximum discrepancies exceed 6 km. Furthermore, the agreement between model-predicted and seismically derived crustal thickness gives support to local isostasy.

[24] Regarding the mantle lithosphere, there is a remarkable thickening in the area of the Gibraltar Arc and High Atlas. This thickening is expected to cause a significant increase of the lithospheric strength in these areas. The opposite effect is expected from the mantle lithosphere thinning obtained under the Alboran Sea and Algerian basin. Allowing for our simplifying assumptions, our inferred lithospheric structure for the Alboran Sea agrees well with that obtained by *Torné et al.* [2000]. Torné et al. carried out three-dimensional gravity modeling combined with heat flow and elevation modeling using the local isostasy assumption. *Torné et al.* [2000] state that the correspondence between the thickest sediment accumulation and the thinnest crust, and the small residual elevation and gravity anomalies provide evidence for local isostatic compensation.

## 5. Scoring the Quality of Results

[25] In order to choose the best model, we have compared the strain rates and principal directions of stress from each model with seismicity data and observed directions of maximum horizontal compression (Figure 2), respectively. Other potentially testable predictions include fault slip rates and relative velocities between pairs of points. However, a comparison with observations is not yet possible in the study area due to the lack of well-constrained geologic estimates of neotectonic fault slip rates and insufficient accumulation of Global Positioning System (GPS) geodetic data.

[26] To score the model-predicted strain rates, we have followed the procedure described by *Jiménez-Munt et al.* [2001a] to calculate a correlation coefficient between seismic strain rate and the modeled maximum principal strain rate. The seismic strain rate at a given point is proportional to the sum of scalar seismic moments of all the earthquakes in the area, averaged with a moving Gaussian filter. To avoid border effects we have considered events occurring in an area larger than that modeled. The scalar seismic moment was computed from the body wave magnitude $m_b$. We are not attempting to compare absolute values of seismic and modeled strain rates, but only their relative variations. The reason for this is that it is uncertain what fraction of the anelastic strain is expressed as earthquakes, even within the brittle or frictional upper parts of the lithosphere.

[27] We have also computed the mean misfit (in degrees) between observed and model-predicted azimuths of the most compressive horizontal principal stress. Data are weighted depending on their quality, with weights changing from 1 to 5 (corresponding to qualities E to A, respectively). Since the misfit cannot exceed 90°, an average misfit higher than 45° means no correlation, or anticorrelation, between the model and the data. On the other hand, the inherent high scatter of stress data (Figure 2) indicates that the average misfit will always be high, normally exceeding about 25°. Therefore, keeping in mind the small range of expected values of the misfit, we can infer that even small variations of the average misfit might be significant to discriminate between different models.

## 6. Results

[28] In the first series of numerical experiments performed (model set 1) we have used the set of faults shown in Figure 4 and have varied the fault friction coefficient. Figure 7 shows the model-predicted long-term average fault

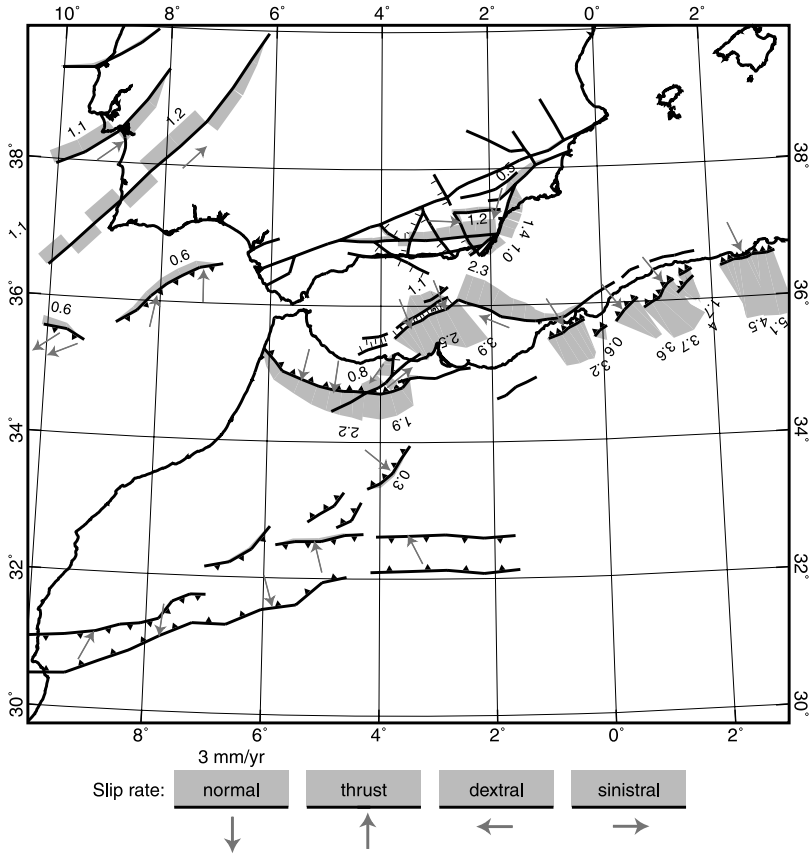


**Figure 7.** Fault slip rates (mm $yr^{-1}$) obtained with the fault network of model set 1 and a fault friction coefficient $f_f = 0.05$ Small gray arrows in hanging walls show the directions of slip. Unlabeled faults have slip rates so low that they are probably numerical artifacts and should be considered as inactive.

slip rates assuming a fault friction coefficient of 0.05. Grey arrows indicate the slip directions of faults. The general trend of modeled fault slip directions is consistent with geological indications [e.g., *Instituto Geográfico Nacional*, 1992]. Vertical NE-SW striking faults are predicted to have sinistral motion (e.g., the Alhama-Palomares-Carboneras fault system and the SW end of the Nekor fault), while E-W to NW-SE striking faults are predicted to have dextral motion (e.g., Alpujarra corridor and the Nerja and Yussuf basin faults). Shortening is mainly accommodated in this model by thrust faults of the Tell cordillera, Rif front, and faults bordering the Alboran Ridge.

[29] Computed fault slip rates in the western Iberian Peninsula are of the order of 1 mm $yr^{-1}$. These values are significantly higher than those obtained in the neotectonic models by *Jiménez-Munt et al.* [2001b], which produced maximum slip rates of 0.2 mm $yr^{-1}$. A possible explanation for this discrepancy is that in their models, which extend from Gibraltar to the Azores region, plate convergence is not transferred to these faults, but is mainly accommodated farther to the south, along the modeled Azores-Gibraltar segment of the plate boundary. This discrepancy highlights the significant influence of the submarine fault network west of Gibraltar on computed slip rates on faults in land. More data on marine geophysics to better constrain offshore faults and trenching studies of onshore faults are needed to reduce uncertainty about the level of seismic hazard for these onshore faults in western Iberia.

[30] A somewhat surprising result is that computed slip rates on the thrust faults of the Atlas Mountains are very low (actually, within the range which may be attributed to numerical approximation in the finite element program). *Gómez et al.* [2000] infer shortening of as much as 15 to 36 km in the High Atlas since middle Miocene. If this shortening occurred at a constant rate, we would expect to see rates of 1 to 2 mm $yr^{-1}$ today, and neotectonic models by *Jiménez-Munt et al.* [2001b] predict rates of up to 1.8 mm $yr^{-1}$. The reason for the lower rates here is that the active thrust fault traces have been represented in more detail, including the apparent restraining gaps between them. Simultaneously, a more detailed model of the Alboran region has increased the tectonic degrees of freedom outside the Atlas. It remains to be resolved which approximation of this range is superior; future geodetic data will be extremely useful in this effort.

[31] The area of highest fault slip rates is northern Algeria, with shortening rates of 2.5∼4.5 mm $yr^{-1}$ (obtained by multiplying the fault slip rates by cos 25°). These high rates are consistent with the strong seismic activity of this area. On the contrary, the relatively high shortening rates predicted along the eastern Rif and Alboran Ridge do not agree with the absence of reverse and thrust-related focal mechanisms in the area. Actually, the instrumental seismicity trend in Morocco, with maximum activity in the Alhoceima region, is not directly related to the Alboran Ridge, Nekor fault, or Rif thrust faults. Instead,

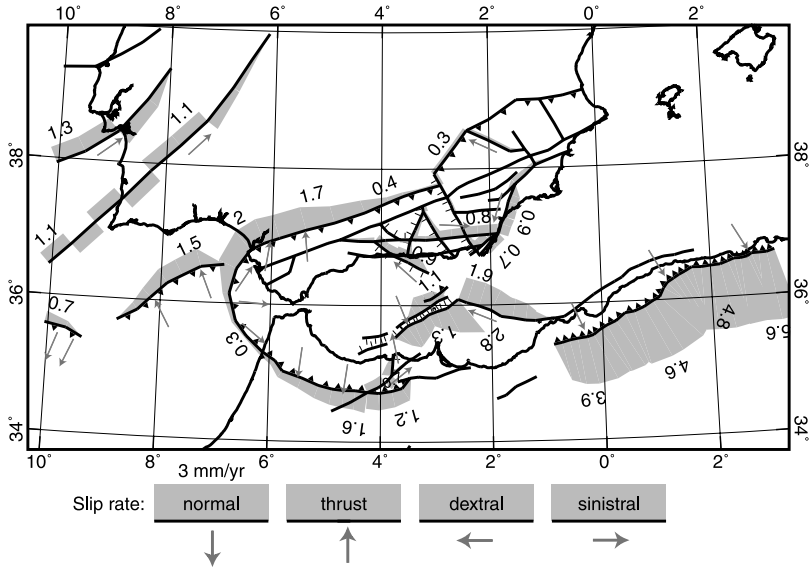


**Figure 8.** Fault slip rates obtained with our most successful model (model set 2, $f_f = 0.05$). Conventions are as in Figure 7.

deformation appears to be occurring over a NE-SW region of distributed shear (Figure 1), along NNE-SSW to N-S oriented faults, which show predominant sinistral strike-slip and normal faulting [e.g., *Hatzfeld et al.*, 1993; *Calvert et al.*, 1997; *Bezzeghoud and Buforn*, 1999].

[32] These results from model set 1 suggest that the Nekor fault is not favorably oriented to become active, in agreement with the absence of significant seismicity and with the lack of evidence of Quaternary slip along its northeastern termination. In contrast, in the Alhoceima region, the N-S striking modeled Trougout fault (Tr in Figure 4) is more favorably oriented and slips in a normal sense with a component of left-lateral motion. Therefore our modeling provides an explanation for the seismicity concentration in minor faults of northern Morocco instead of in long faults with a clear topographic expression such as the Nekor fault.

[33] The Alhoceima region is possibly being fractured to transfer slip from the Rif to the Alboran Ridge. Therefore, if we assume that slip is not occurring aseismically, these areas might be accumulating strain, as also suggested by *Calvert et al.* [1997]. The diffuse SW-NE band of strike-slip earthquakes may represent an embryonic fault. A similar situation can be found in the southern Sierra Nevada range (California), where a band of seismicity connecting the Kern County and Walker Pass earthquakes has been interpreted as a newly forming fault [*Bawden et al.*, 1999]. Focal mechanisms of left-lateral earthquakes in both areas show a counterclockwise rotation of focal planes from the strike of seismic lineament, consistent with slip on shear fractures in the early stages of fault development [*Bawden et al.*, 1999].

[34] Maximum convergence rates of 0.5 mm $yr^{-1}$ are obtained in the fault running along the SE part of the Guadalquivir Bank, in the central Gulf of Cadiz. Therefore model set 1 seems to underestimate the amount of shortening in this area, as indicated by significant seismicity (Figure 1) associated with reverse faulting in the area. The only predicted active fault zones in southern Spain are the Nerja fault and the Alhama-Palomares-Carboneras fault system, whereas the Cadiz-Alicante fault zone remains inactive. Our modeling thus provides an explanation for present-day lack of activity of some faults, such as the Cadiz-Alicante fault zone and the Nekor fault, which had a significant strike-slip movement (dextral in the former and sinistral in the latter) during the Miocene, resulting in the west and WSW transport of the Betics and Rif, respectively [*Sanz de Galdeano*, 1990; *Leblanc*, 1990]. On the other hand, a comparison with seismicity suggests that an important defect of this first model set is that fault slip rates seem to be overestimated in the Rif area, compared to southern Spain and Gulf of Cadiz.

[35] In this first model set we adopted a conservative point of view, in the sense that we only included mapped fault zones. In contrast, in a second finite element grid (model set 2) we have modified the previous fault network by adding interpreted connections between faults beneath marine sediments and young continental alluvium. Figure 7 shows the set of faults included in the grid of model set 2. We have prolonged faults where they are suspected to connect at depth. For instance, we have defined a unique active thrust fault system at the Tell mountains. Of course, this should be interpreted as an end-member situation, since, for simplicity, only a continuous low-angle fault and not small vertical faults are considered in this area. The main novelty of this second grid is that the Betics and Rif are explicitly modeled as the same orogenic belt. Therefore the thrust front in the Betics and Gibraltar areas connects with the Rif front. The shallow compressional structures in the Betics do not define a continuous front because they are either disrupted by later extensional events or buried under the Guadalquivir foreland sediments. Therefore the modeled front should be considered as an idealization representing all the Betic thrusts; it has been placed at an intermediate position between the most external structures, which result from thin-skinned thrusting, and the thrusts bordering the internal units of the mountain belt.

[36] Figure 8 shows predicted fault slip rates obtained with model set 2, assuming a fault friction coefficient of

0.05. Again, the highest slip rates are obtained in northern Algeria, with shortening rates of 3.5∼5 mm $yr^{-1}$. These values must be considered as an upper bound due to the probably exaggerated continuity of the modeled Tell thrust. The main difference with respect to model set 1 is that fault slip is now more homogeneously distributed along the Rif and western Betic thrusts, in better agreement with distributed seismicity in southern Spain and northern Morocco (Figure 1). The shortening rate of the thrust fault bordering the Guadalquivir Bank is increased to 1.4 mm $yr^{-1}$, which is more consistent with seismic activity in the central Gulf of Cadiz. The predicted slip rates do not change significantly in other modeled fault zones. In comparison to the neotectonic studies by *Jiménez-Munt et al.* [2001a, 2001b], where the only faults considered in the Ibero-Maghrebian area were the Betic and Rif thrust fronts, we conclude from this study that including the Alboran Ridge and Yussuf fault permits significant internal transpressive deformation of the Alboran Sea, which therefore is not acting as a rigid microplate, at least in the present-day situation.

[37] The results of testing these two model sets against stress and seismologic data, for different values of fault friction coefficient, are shown in Figure 9. The scores for both data sets, stress-direction and seismicity, clearly favor model set 2 since the misfit of most compressive horizontal stress directions is lower and the correlation with seismic strain rate is higher than for model set 1.

[38] Figure 9 also shows the results of a parametric study, performed using the fault network of model set 2, to evaluate the influence of the rheologic parameters. The importance of varying the creep activation energy $Q$ is that it determines the amount of coupling between the upper crust and the upper mantle across the lower crust. A high value of $Q$ means a strength decrease in the lower crust, and the upper crust is decoupled, whereas a low value of $Q$ means a strong coupling to the upper mantle. The parametric study shows that results are less sensitive to the rheologic parameters than to the assumed fault network and variations of the fault friction coefficients. Comparing the pattern of scores of both data sets we infer that the best fit is achieved with $Q$ = 200 kJ $mol^{-1}$ and a fault friction coefficient value as low as 0.04–0.06. When this coefficient is increased, slip is mainly concentrated on long thrust faults, and most faults in the Betics and Alboran Sea become inactive. The optimum fault friction coefficient is much lower than the typical value of 0.85 assumed for the internal friction coefficient of blocks between faults. This result is consistent with previous models reporting low friction coefficients on faults: in California [*Bird and Kong*, 1994], Alaska [*Bird*, 1996], Asia [*Kong and Bird*, 1996], and globally [*Bird*, 1998]. *Jiménez-Munt et al.* [2001b] obtained a fault friction coefficient of 0.10–0.15 for the Azores-Gibraltar system. The lower values obtained in this study suggest a lower strength of faults in the continental domain with respect to the oceanic transform boundary. A possible explanation of the low strength of faults involves anomalous pore pressure, possibly caused by upflow of subducted water from the lower crust or mantle [*Bird and Kong*, 1994].

[39] In order to find out which is the critical difference between model sets 1 and 2, we have tested a model with fault friction coefficient of 0.05 and the fault network of model set 1 except with the modification that the Betic and Rif thrust fronts are connected. Both seismicity and stress orientation data are significantly better fit when introducing this change. Misfit of stress directions is reduced from 29.63 to 28.7 and the seismic correlation coefficient is increased from 0.524 to 0.548. The reason for this improvement is that fault slip is more homogeneously distributed between the Rif, Betics, and Guadalquivir Bank thrusts. Modeling the Tell mountains front as a continuous thrust fault induces further improvement of data fitting to reach the scoring results of the best model of model set 2 (Figure 9; $Q$ = 200 kJ $mol^{-1}$ and fault friction 0.05). Therefore both changes are shown to be preferred by data, thus suggesting that faults might be more continuous at depth than surface geologic maps imply.

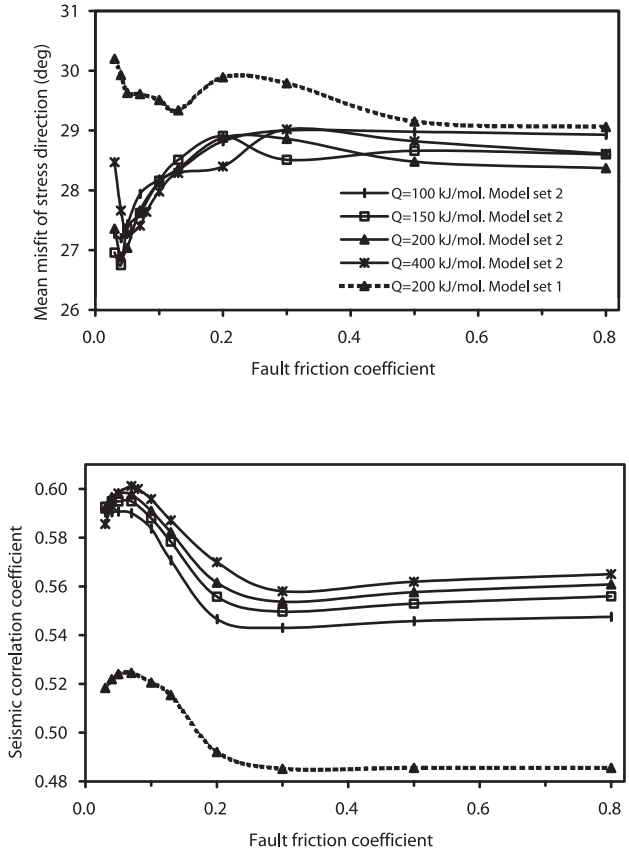


**Figure 9.** Results of testing two models based on different fault networks, against (top) seismicity distribution and (bottom) stress direction data. Best results are obtained with the fault network of model set 2 and a fault friction coefficient of ∼0.05.

[40] The results obtained from the best model are shown in Figures 9, 10, 11, and 12. Figure 10 shows surface velocities relative to the Eurasia plate. In the eastern part of the modeled area, most convergence is absorbed in the area of the Tell mountains front. In contrast, farther to the west, convergence is distributed between northern Morocco, the Alboran Sea, and southern Spain. A general characteristic of the predicted velocity distribution is the increase of the westward component of the velocity from east to west. This increase is particularly significant when moving from the Algerian basin toward the Gibraltar Arc. Following model

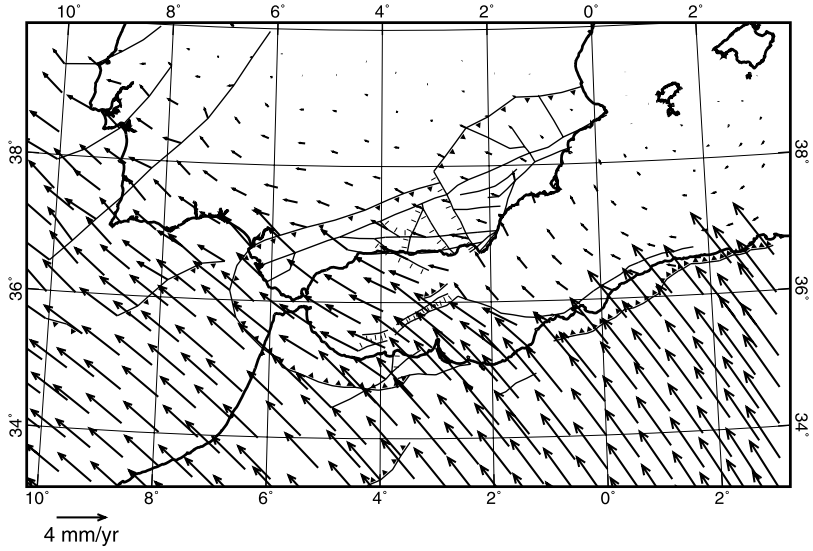


**Figure 10.** Predicted velocities (with respect to Europe) in the Ibero-Maghrebian region, from model set 2 with $f_f = 0.05$. The reference point for each velocity vector is located at the tail. Some symbols have been omitted for clarity.

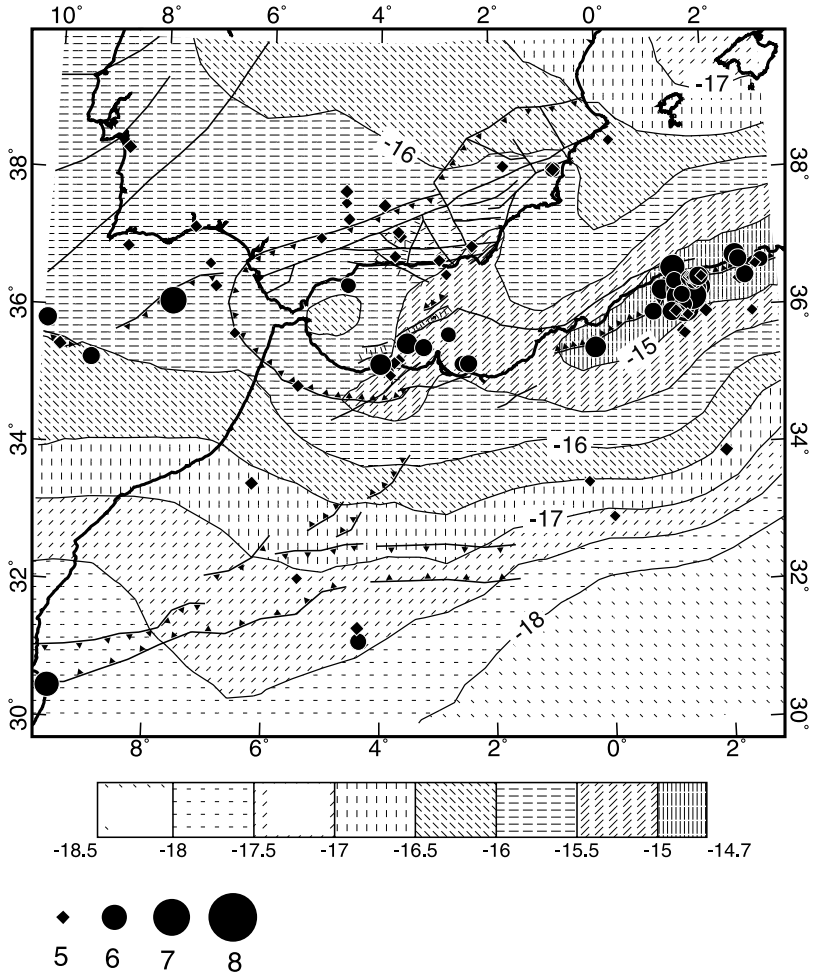


**Figure 11.** Common logarithms of smoothed strain rate ($s^{-1}$) predicted by model set 2 with $f_f = 0.05$. To enable comparison with seismic strain rate, we also show the epicenters of shallow earthquakes of magnitude 5 or greater, in the period 1910–1999.

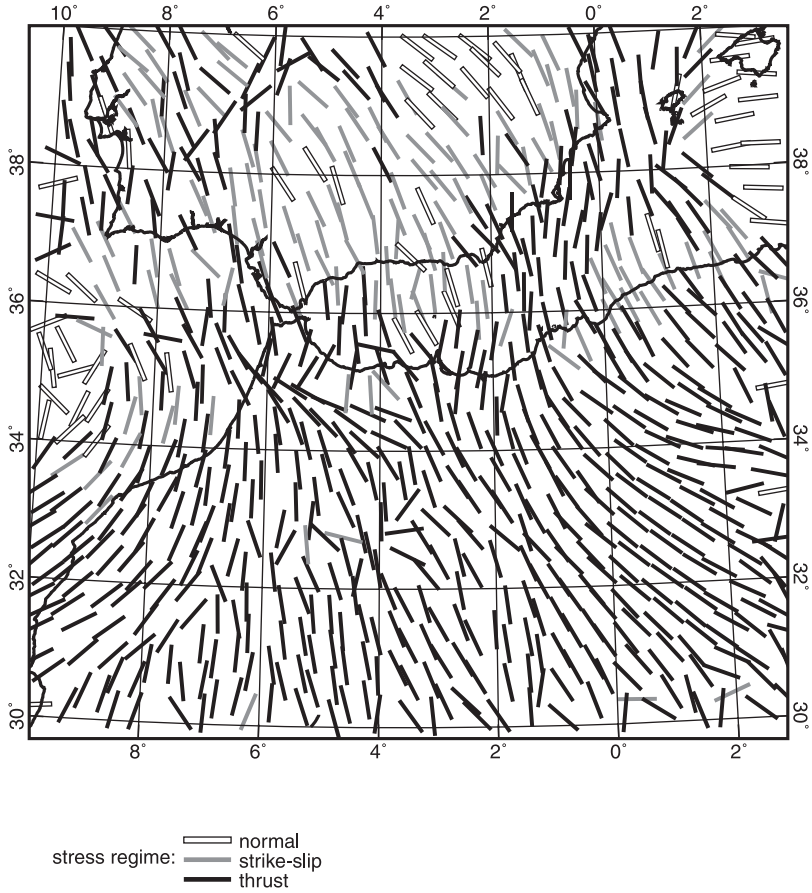


**Figure 12.** Most compressive horizontal principal stress orientations and stress regime predicted by the best model of model set 2 (with $f_f = 0.05$). Some symbols have been omitted for clarity.

results, the Alboran domain is presently escaping in WNW direction, with a velocity of about 3 mm $yr^{-1}$ with respect to stable Europe.

[41] The neotectonic study by *Jiménez-Munt et al.* [2001a, 2001b] obtained the best fit of observations when applying to the eastern end of the Alboran Sea a westward velocity of 2.6 mm $yr^{-1}$. With this boundary condition Jiménez-Munt and coauthors forced both the south Iberian and north African margins to act as plate boundaries and the Alboran domain to behave as an independent microplate between the two major plates. In the present model, which is more detailed for the Alboran region and extends to Algeria, we obtain the westward motion of the Alboran domain without the need for imposing any velocity condition there, but it is associated with lateral extrusion due to plate convergence. Therefore our results give further support to the bifurcation of the plate boundary in the Ibero-Maghrebian region. However, unlike the model by *Jiménez-Munt et al.* [2001a, 2001b], our model has significant strain within the Alboran Sea as well as in the Betic-Rif orogen.

[42] This neotectonic model provides a rough estimate of the contribution of plate convergence to the westward motion of the Alboran domain. It can be deduced that the rapid westward motion of the Alboran domain during the Miocene, with a total westward displacement of 400–500 km [*Sanz de Galdeano*, 1990], was not entirely caused by lateral expulsion related to plate convergence. Therefore another mechanism causing westward movement of the Alboran domain must be invoked to explain the Neogene evolution of the area. *Lonergan and White* [1997] have proposed that this mechanism could be the westward migration of a west-vergent subduction zone relative to both Africa and Eurasia. Actually, three-dimensional neotectonic modeling of the southern Tyrrhenian subduction shows that a combination of plate convergence and slab roll-back (acting at nearly right angles] increases significantly the velocity of the upper plate toward the trench [*Negredo et al.*, 1999].

[43] Our results are not consistent with the present-day geodynamic scenario envisaged by *Rebaï et al.* [1992]. These authors use a reconstruction of the modern stress field in the Mediterranean region to deduce a westward expulsion of the Alboran domain accommodated by right-lateral motion of the Cadiz-Alicante fault and left lateral motion on what the authors term the Nekor-Carboneras-Alicante fault. In contrast, we do not obtain significant slip along the Cadiz-Alicante or Nekor faults.

[44] Figure 11 shows the common logarithm of the smoothed strain rate obtained in the best model of set 2. For qualitative comparison with the seismic strain rate we also display shallow earthquakes with magnitude 5 or greater (during 1910–1999). The smoothed strain rate includes both the contributions from anelastic deformation within the continuum blocks and those from fault slip, but does not include transient elastic strain. The area of maximum model-predicted strain rate coincides with the area of

maximum seismic activity in northern Algeria. Also the relatively high strain rate in the southern Alboran Sea and northeastern Morocco is very consistent with the significant seismicity in these areas. In the region extending from the eastern Rif to the western Tell mountains, the high predicted strain rates are due to internal deformation of continuum blocks. Since this deformation can be interpreted as related to all faults too small to appear in our grid, this result is in good agreement with activity of subsidiary faults, such as those responsible for the seismicity in the Alhoceima region.

[45] Figure 12 shows the model-predicted directions of maximum horizontal compression. This model properly reproduces the regional trend of N-S to NW-SE compression, in agreement with geologic and seismotectonic studies [*Rebaï et al.*, 1992; *Ribeiro et al.*, 1996; *Buforn et al.*, 1995; *Herraiz et al.*, 2000]. The stress regime changes, from west to east, from thrusting in the Tell cordillera to predominant strike-slip and normal faulting in the Betics, central Alboran Sea, and Rif mountains. Several authors [e.g., *Calvert et al.*, 1997; *Bezzeghoud and Buforn*, 1999] have previously deduced this major change of stress regime on the basis of the analysis of source mechanisms of earthquakes in the Ibero-Maghrebian region. Our study reveals that the distinct styles of deformation in the two regions can be explained by different fault geometries and lithospheric structure, instead of being ascribed to possible ongoing subcrustal processes (subduction or delamination).

[46] The presence of a region of normal-type stress field in the central Betics, which is larger in model set 2 than in model set 1, agrees qualitatively with the inference of *Galindo-Zaldívar et al.* [1999], reporting present-day NE-SW extension in the Granada Basin (GB in Figure 4). However, the model-predicted rates of extension on normal faults in this area never exceed 0.1 mm $yr^{-1}$. In order to obtain a rough estimate of extension rates we have used the seismic moments of normal-faulting earthquakes in the catalog. We have considered normal-faulting earthquakes with magnitude equal or higher than 4 (5 being the highest magnitude). We have added up their scalar seismic moments (estimated from magnitudes), then divided by total length of all normal faults ($\sim$300 km), by estimated depth to the brittle-ductile transition (15 km), and by a typical shear modulus ($32 \times 10^9$ N $m^{-2}$). This calculation yields a mean slip rate of 0.04 mm $yr^{-1}$; therefore we can infer that model-predicted rates of extension are roughly correct (within an order of magnitude).

## 7. Conclusions

[47] In the present study we have compared conservative and interpretative finite element models for simulating the neotectonics of the Ibero-Maghrebian region. The latter model has been shown to properly reproduce the main characteristics of present-day stress and strain field in the area. We show with this model that the connection between the Betics and Rif cordilleras and the continuity of the thrust faults of the Tell mountains are features required by observations. Both features indicate that faults might be more continuous at depth than geologic maps show.

[48] Model predictions of strain rate and vertically integrated stresses are compared to seismicity and stress direction data, resulting in an optimal fault friction coefficient as low as 0.05. This value is consistent with the fault weakness previously found in regional and global neotectonic models.

[49] The area of highest fault slip rates predicted by the best model corresponds to northern Algeria, the most seismically active area in the Ibero-Maghrebian region. Farther to the west, fault slip is more homogeneously distributed over southern Spain, the Gulf of Cadiz, northern Morocco, and the Alboran Sea. This result gives support to the idea of a diffuse plate boundary in the area. Model results indicate that the Alboran Sea undergoes significant internal transpressive deformation, so it is not presently acting as a rigid microplate. The western part of the basin and the Betic-Rif chain are presently escaping in WNW direction with velocity of about 3 mm $yr^{-1}$ with respect to the Eurasia plate. This result indicates that lateral expulsion associated with plate convergence cannot account for much more rapid westward motion of these areas during the Miocene.

[50] The Cadiz-Alicante and Nekor fault zones, which are thought to have accommodated significant westward motion of the Alboran domain during the Miocene, are shown to be unfavorably oriented with respect to the present-day stress field. On the other hand, the NNE-SSW orientation of subsidiary faults responsible for recent seismicity in the Alhoceima region is shown here to be favorable for left-lateral motion. Furthermore, the best model predicts a high strain rate for this area.

[51] In agreement with seismotectonic studies of the Ibero-Maghrebian area, our modeling reproduces a major change of the stress regime, from thrust faulting in northern Algeria to predominant strike-slip and normal faulting in the Betic-Rif chain.

[52] Most of results obtained with this modeling should be considered as predictions that are testable by future data-gathering, in particular by geological fault slip rate estimation and geodetic observations. In fact, ongoing research projects will soon provide high-accuracy Global Positioning System measurements of the present-day pattern of crustal deformation in this region.

[53] **Acknowledgments.** The authors are very grateful to J. Freymueller, P. Elosegui, and an anonymous reviewer for their constructive revision of the manuscript. Spanish research programs Ramón y Cajal, BTE2002-02462, REN2000-0777-C02-01/RIES, DGESIC PB97-1267-C03-01, and a grant from the Foundation Jaime del Amo (University Complutense of Madrid) have partially supported this work. F. Vidal, from the Instituto Geográfico Nacional (IGN), kindly provided seismic catalogue. The authors are very grateful to I. Jiménez-Munt (University of Milan), A. Udías, M. Osete (University Complutense of Madrid), E. Gràcia (Institute of Earth Sciences 'J. Almera'-CSIC Barcelona), F. Gómez (University of Cornell), and Z. Liu (University of California, Los Angeles) for constructive comments.

## References

Alvarez-Marrón, J., Pliocene to recent structure of the eastern Alboran Sea (W Mediterranean), *Proc. Ocean Drill. Program Sci. Results*, *161*, 345–355, 1999.

Andrieux, J., J. M. Fontobé, and M. Durand-Delga, Sur un modèle explicatif de l'Arc de Gibraltar, *Earth Planet. Sci. Lett.*, *12*, 191–198, 1971.

Argus, D. F., R. G. Gordon, C. DeMets, and S. Stein, Closure of the Africa-Eurasia-North America plate motion circuit and tectonics of the Gloria fault, *J. Geophys. Res.*, *94*, 5585–5602, 1989.

Balanyá, J. C., and V. García-Dueñas, Les directions structurales dans le Domaine d'Alboran de part et d'autre du Détroit de Gibraltar, *C.R. Acad. Sci., Ser. 2*, *304*, 929–932, 1987.

Banda, E., Crustal parameters in the Iberian Peninsula, *Phys. Earth Planet. Inter.*, *51*, 222–225, 1988.

Banda, E., J. Gallart, V. García-Dueñas, J. Dañobeitia, and J. Makris, Lateral variation of the crust in the Iberian Peninsula: New evidence for the Betic Cordillera, *Tectonophysics*, *221*, 53–66, 1993.

Bawden, G. W., A. J. Michael, and L. H. Kellogg, Birth of a fault: Connecting the Kern County and Walker Pass, California, earthquakes, *Geology*, *27*, 601–604, 1999.

Bezzeghoud, M., and E. Buforn, Source parameters of the 1992 Melilla (Spain, $M_w$ = 4.8), 1994 Alhoceima (Morocco, $M_w$ = 5.8), and Mascara (Algeria, $M_w$ = 5.7) earthquakes and seismotectonic implications, *Bull. Seismol. Soc. Am.*, *89*, 359–372, 1999.

Bezzeghoud, M., A. Ayadi, A. Sébaï, M. Aït Messaoud, A. Mokrane, and H. Benhallou, Seismicity of Algeria between 1365 and 1989: Map of maximum observed intensities (MOI), in *Avances en Geofísica y Geodesia*, vol. I, pp. 107–114, Inst. Geogr. Nac., Madrid, 1996.

Bird, P., Computer simulations of the Alaskan neotectonics, *Tectonics*, *15*, 235–236, 1996.

Bird, P., Testing hypotheses on plate-driving mechanisms with global lithosphere models including topography, thermal structure, and faults, *J. Geophys. Res.*, *103*, 10,115–10,129, 1998.

Bird, P., Thin-plate and thin-shell finite element programs for forward dynamic modeling of plate deformation and faulting, *Comput. Geosci.*, *25*, 383–394, 1999.

Bird, P., and X. Kong, Computer simulations of California tectonics confirm very low strength of major faults, *Geol. Soc. Am. Bull.*, *106*, 159–174, 1994.

Buforn, E., A. Udias, and R. Madariaga, Intermediate and deep earthquakes in Spain, *Pure Appl. Geophys.*, *136*, 375–393, 1991.

Buforn, E., C. Sanz de Galdeano, and A. Udias, Seismotectonics of the Ibero-Maghrebian region, *Tectonophysics*, *248*, 247–261, 1995.

Calvert, A., F. Gómez, D. Seber, N. J. Barazangi, A. Ibenbrahim, and A. Demnati, An integrated geophysical investigation of recent seismicity in the Al-Hoceima Region of North Morocco, *Bull. Seismol. Soc. Am.*, *87*, 637 –651, 1997.

Calvert, A., E. Sandvol, D. Seber, M. Barazangi, S. Roecker, T. Mourabit, F. Vidal, G. Alguacil, and N. Jabour, Geodynamic evolution of the lithosphere and upper mantle beneath the Alboran region of the western Mediterranean: Constraints from travel time tomography, *J. Geophys. Res.*, *105*, 10,871–10,898, 2000.

Choubert, G., M. M. P. Fallot, J. Marcais, G. Suter, and R. Tilloy, Carte geologique du Maroc (1:500,000), Serv. Geol., Div. des Mines et de la Geol., Dir. de la Prod. Ind. et des Mines, Prot. de la Repub. Fr. au Maroc, Paris, 1955.

Chung, W. Y., and H. Kanamori, Source process and tectonic implications of the Spanish deep-focus earthquake of March 29, 1954, *Phys. Earth Planet. Inter.*, *13*, 85–96, 1976.

Comas, M. C., V. García-Dueñas, and M. J. Jurado, Neogene tectonic evolution of the Alboran Basin from MCS data, *Geo Mar. Lett.*, *12*, 157–164, 1992.

Comas, M. C., J. P. Platt, J. I. Soto, and A. B. Watts, The origin and tectonic history of the Alboran Basin: Insights from Leg 161 results, *Proc. Ocean Drill. Program Sci. Results*, *161*, 555–580, 1999.

De Larouzière, F. D., J. Bolze, P. Bordet, J. Hernandez, C. Montenat, and P. Ott dÉstevou, The Betic segment of the lithospheric trans-Alboran shear zone during the late Miocene, *Tectonophysics*, *152*, 41–52, 1988.

DeMets, C., R. G. Gordon, D. F. Argus, and S. Stein, Current plate motions, *Geophys. J. Int.*, *101*, 425–478, 1990.

Docherty, J. I. C., and E. Banda, Evidence for the eastward migration of the Alboran Sea based on regional subsidence analysis: A case for basin formation by delamination of the subcrustal lithosphere?, *Tectonics*, *14*, 804–818, 1995.

Fernàndez, M., I. Marzán, A. Correia, and E. Ramalho, Heat flow, heat production, and lithospheric thermal regime in the Iberian Peninsula, *Tectonophysics*, *291*, 29–53, 1998.

Frizon de Lamotte, D., Un example de collage synmetamorphe: La déformation miocène des Temsamane (Rif externe, Maroc), *Bull. Soc. Geol. Fr.*, *3*, 337–344, 1987.

Galindo-Zaldívar, J., A. Jabaloy, I. Serrano, J. Morales, F. González-Lodeiro, and F. Torcal, Recent and present-day stresses in the Granada Basin (Betic cordilleras): Example of a late Miocene-present-day extensional basin in a convergent plate boundary, *Tectonics*, *18*, 686–702, 1999.

García-Dueñas, V., J. M. Martínez-Martínez, M. Orozco, and J. I. Soto, Plis-nappes, cisaillements syn-à post-metamorphiques et cisaillements ductiles-fragiles en distension dans les Nevado-Filábrides (Cordillères Bétiques, Espagne), *C. R. Acad. Sci.*, *307*, 1389–1395, 1988.

García-Dueñas, V., J. C. Balanyá, and J. M. Martínez-Martínez, Miocene extensional detachments in the outcropping basement of the northern Alboran basin (Betics) and their tectonic implications, *Geo Mar. Lett.*, *12*, 88–95, 1992.

Gómez, F., W. Beauchamp, and M. Barazangi, Role of the Atlas Mountains (northwest Africa) within the African-Eurasian plate-boundary zone, *Geology*, *28*, 775–778, 2000.

Gràcia, E., J. J. Dañobeitia, J. Vergés, R. Bartolomé, and D. Córdoba, The structure of the Gulf of Cadiz (SW Iberia) imaged by new multi-channel seismic reflection data (abstract), *Geophys. Res. Abstr.*, *2*, 61, 2000.

Grimison, N. L., and W.-P. Chen, The Azores-Gibraltar plate boundary: Focal mechanisms, depths of earthquakes, and their tectonic implications, *J. Geophys. Res.*, *91*, 2029–2047, 1986.

Hatzfeld, D., and The Working Group for Deep Seismic Sounding, Crustal seismic profiles in the Alboran Sea-Preliminary results, *Pure Appl. Geophys.*, *116*, 167–180, 1978.

Hatzfeld, D., V. Caillot, T.-E. Cherkaoui, H. Jebli, and F. Medina, Microearthquake seismicity and fault plane solutions around the Nekor strike-fault, Morocco, *Earth Planet. Sci. Lett.*, *120*, 31–41, 1993.

Herraiz, M., et al., The recent (upper Miocene to Quaternary) and present tectonic stress distributions in the Iberian Peninsula, *Tectonics*, *19*, 762–786, 2000.

Instituto Geográfico Nacional, Análisis sismotectónico de la Península Ibérica, Baleares y Canarias, scale 1:1,000,000, *Tech. Publ. 26*, Madrid, 1992.

Jiménez-Munt, I., M. Fernàndez, M. Torné, and P. Bird, The transition from linear to diffuse plate boundary in the Azores-Gibraltar region: Results from a thin-sheet model, *Earth Planet. Sci. Lett.*, *192*, 175–189, 2001a.

Jiménez-Munt, I., P. Bird, and M. Fernàndez, Thin-shell modeling of neotectonics in the Azores-Gibraltar region, *Geophys. Res. Lett*, *28*, 1083–1086, 2001b.

Kirby, S. H., Rheology of the lithosphere, *Rev. Geophys.*, *21*, 1458–1487, 1983.

Kong, X., Numerical modeling of the neotectonics of Asia: A new spherical shell finite element method with faults, Ph.D. thesis, Univ. of Calif., Los Angeles, 1995.

Kong, X., and P. Bird, SHELLS: A thin-plate program for modeling neotectonics of regional or global lithosphere with faults, *J. Geophys. Res.*, *100*, 22,129–22,131, 1995.

Kong, X., and P. Bird, Neotectonics of Asia: Thin-shell finite-element models with faults, in *Tectonic Evolution of Asia*, edited by A. Yin and T. M. Harrison, pp. 18–34, Cambridge Univ. Press, New York, 1996.

Leblanc, D., Tectonic adaptation of the External Zones around the curved core of an orogen: The Gibraltar Arc, *J. Struct. Geol.*, *12*, 1013–1018, 1990.

Leblanc, D., and P. Olivier, Role of strike-slip faults in the Betic Rifian Orogeny, *Tectonophysics*, *101*, 344–355, 1984.

Lonergan, L., and N. White, Origin of the Betic-Rif mountain belt, *Tectonics*, *16*, 504–522, 1997.

Maldonado, A., L. Somoza, and L. Pallarés, The Betic orogen and the Iberian-African boundary in the Gulf of Cadiz: Geological evolution (central North Atlantic), *Mar. Geol.*, *155*, 9–43, 1999.

Meghraoui, M., J. L. Morel, J. Andrieux, and M. Dahmani, Tectonique plio-quaternaire de la chaîne tello-rifaine et de la mer d'Alboran: Une zone complexe de convergence continent-continent, *Bull. Soc. Geol. Fr.*, *167*, 141–157, 1996.

Mézcua, J., and J. Rueda, Seismological evidence for a delamination process in the lithosphere under the Alboran Sea, *Geophys. J. Int.*, *129*, F1–F8, 1997.

Morales, J., I. Serrano, F. Vidal, and F. Torcal, The depth of the earthquake activity in the Central Betics (southern Spain), *Geophys. Res. Lett.*, *24*, 3289–3292, 1997.

Mueller, B., J. Reinecker, O. Heidbach, and K. Fuchs, The 2000 release of the World Stress Map, 2000. (Available online at www.world-stress-map.org)

Negredo, A. M., R. Sabadini, G. Bianco, and M. Fernàndez, Three-dimensional modelling of crustal motions caused subduction and continental convergence in the central Mediterranean, *Geophys. J. Int.*, *136*, 261–274, 1999.

Platt, J. P., and R. L. M. Vissers, Extensional collapse of the thickened continental lithosphere: A working hypothesis for the Alboran Sea and Gibraltar Arc, *Geology*, *17*, 540–543, 1989.

Pollack, H. N., S. J. Hurter, and J. R. Johnson, Heat flow from the Earth's interior: Analysis of the global data set, *Rev. Geophys.*, *31*, 267–280, 1993.

Polyak, B. G., et al., Heat flow in the Alboran Sea (the western Mediterranean), *Tectonophysics*, *263*, 191–218, 1996.

Rebaï, S., H. Philip, and A. Taboada, Modern tectonics stress field in the Mediterranean region: Evidence for variation in stress directions at different scales, *Geophys. J. Int.*, *110*, 106–140, 1992.

Ribeiro, A., J. Cabral, R. Baptista, and L. Matias, Stress pattern in Portugal mainland and the adjacent Atlantic region, West Iberia, *Tectonics*, *15*, 641–659, 1996.

Royden, L. H., Evolution of retreating subduction boundaries formed during continental collision, *Tectonics*, *12*, 629–638, 1993.

Sanz de Galdeano, C., Los accidentes y principales fracturas de las Cordilleras Béticas, *Estud. Geol.*, *39*, 157–165, 1983.

Sanz de Galdeano, C., Geologic evolution of the Betic Cordilleras in the western Mediterranean, Miocene to the present, *Tectonophysics*, *172*, 107–119, 1990.

Sanz de Galdeano, C., The E-W segments of the contact between the external and internal zones of the Betic and Rif Cordilleras and the E-W corridors of the internal zone (a combined explanation), *Estud. Geol.*, *52*, 123–136, 1996.

Sanz de Galdeano, C., and J. Vera, Stratigraphic record and paleogeographical context of the Neogene basins in the Betic Cordillera Spain, *Basin Res.*, *4*, 21–36, 1992.

Seber, D., M. Barazangi, A. Ibenbrahim, and A. Demnati, Geophysical evidence for lithospheric delamination beneath the Alboran Sea and Rif-Betic mountains, *Nature*, *379*, 785–790, 1996.

Torné, M., M. Fernàndez, M. C. Comas, and J. I. Soto, Lithospheric structure beneath the Alboran Basin: Results from three-dimensional gravity modeling and tectonic relevance, *J. Geophys. Res.*, *105*, 3209–3228, 2000.

Tortella, D., M. Torné, and A. Pérez-Estaún, Geodynamic evolution of the eastern segment of the Azores-Gibraltar zone: The Gorringe Bank and the Gulf of Cadiz region, *Mar. Geophys. Res.*, *19*, 211–230, 1997.

Udías, A., A. López-Arroyo, and J. Mézcua, Seismotectonics of the Azores-Alboran region, *Tectonophysics*, *31*, 259–289, 1976.

Vissers, R. L., J. P. Platt, and D. Van der Wal, Late orogenic extension of the Betic Cordillera and the Alboran Domain: A lithospheric view, *Tectonics*, *14*, 786–803, 1995.

Watts, A. B., J. P. Platt, and P. Buhl, Tectonic evolution of the Alboran Sea Basin, *Basin Res.*, *5*, 153–177, 1993.

Zoback, M. L., First- and second-order patterns of stress in the lithosphere: The World Stress Map project, *J. Geophys. Res.*, *97*, 11,703–11,728, 1992.

P. Bird, Department of Earth and Space Sciences, University of California, Los Angeles, CA 90095-1567, USA. (pbird@ess.ucla.edu)

E. Buforn and A. M. Negredo, Departamento de Geofísica, Facultad de Física, Universidad Complutense de Madrid, E-28040 Madrid, Spain.

C. Sanz de Galdeano, Instituto Andaluz de Ciencias de la Tierra, Consejo Superior de Investigaciones Científicas-Universidad de Granada, Granada, Spain.